**Supplementary data**

**Methods and Materials:**

*Mice*

Wild type C57BL/6 (strain# 00064) and BALB/c (strain# 000651) mice were purchased from Jackson Laboratory (Bar Harbor, ME). *hLRRC32*$^{KI}$ mice in C57BL/6 background was generated by Ingenious targeting laboratory (Ronkonkoma, NY). Age- and sex-matched mice were used for all the *in vivo* experiments. All experimental animals were 6-11 weeks old.

*Cell lines and mice*

Jurkat, 4T1, MB-49 with hGARP overexpression were described previously [1]. Cancer cells were authenticated by gene expression analysis, *in vivo* growth and histology. MB-49 urothelial carcinoma cell line was kindly provided by Dr. Xue Li (Cedars-Sinai Medical Center, Los Angeles, CA). 293FT and LLC1 lines were purchased from ATCC (Manassas, VA). CMT-167 cell line was obtained from Sigma (St. Louis, MO). All cell lines were tested to be free of *Mycoplasma* by PCR. For all the *in vivo* tumor experiment, tumor cells were used within the first four passages of the culture.

*Generation of human/mouse GARP-expression vectors*

Human and mouse GARP was amplified by PCR and subcloned between the BglII and HpaI sites in a MigR1 retroviral vector as previously described [1].

For chimeric construction, we used the following primers:

20-60 Forward: GCT CTC TAC TTG TCC GGG AAC CAA CTG CGG AGT ATC CTG GCC TCA CCC

20-60 reverse: GGG TGA GGC CAG GAT ACT CCG CAG TTG GTT CCC GGA CAA GTA GAG AGC

61-100 forward: CAG GCC CTG CCC TAC CTG GAG CAC CTC AGC CTG GCT CAC AAC CGG CTG

61-100 reverse: CAG CCG GTT GTG AGC CAG GCT GAG GTG CTC CAG GTA GGG CAG GGC CTG

101-140 forward: AAC AGC CTG CAT GGC AAT CTG GTG GAG CGG CTG CTG GGG GAG GCA CCC

101-140 reverse: GGG TGC CTC CCC CAG CAG CCG CTC CAC CAG ATT GCC ATG CAG GCT GTT

141-170 forward: CGC CTG GCA CGC CAC ACC TTC TGG GAC ATG CCT GCG CTG GAG CAG CTT

141-170 reverse: AAG CTG CTC CAG CGC AGG CAT GTC CCA GAA GGT GTG GCG TGC CAG GCG

171-207 forward: ACT CAC CTC AAT CTC TCC AGA AAC TCC CTC ACC TGC ATC TCC GAC TTC

171-207 reverse: GAA GTC GGA GAT GCA GGT GAG GGA GTT TCT GGA GAG ATT GAG GTG AGT

208-265 forward: TTC CCT GAC CTG GCC GTG TTC CCG AGA CTC ATC TAC CTG AAC TTG TCC

208-265 reverse: GGA CAA GTT CAG GTA GAT GAG TCT CGG GAA CAC GGC CAG GTC AGG GAA

266-322 forward: AAT GAG ATC GAA CTG GTC CCT GCT AGC TTT CTT GAG CAC CTG ACC TCC

266-322 reverse: GGA GGT CAG GTG CTC AAG AAA GCT AGC AGG GAC CAG TTC GAT CTC ATT

All constructs were subcloned into MigR1 retroviral vector for retrovirus production as previously reported[1]. The efficiency of mutagenesis was assessed by DNA sequencing. Chimeric constructions were transfected into 293FT cells and the cells with desired expression level of the construct were selected by FACS sorting.

*In vivo Murine tumor model*

LLC1 tumor cells ($5\times10^5$) or CMT-167 cells ($1\times10^5$) were injected s.c. on the right flank of *hLRRC32*$^{KI}$ female mice. Mice were given PIIO-1 (200 μg), anti-PD-1 (100 μg) or combination of both on day 8 every three days for 4 treatments. Tumor growth was monitored, and tissues were collected on day 18. Flow cytometry were analyzed at the end point of the experiment.

MB-49-hGARP or -EV tumor cells ($1\times10^5$) were injected s.c. in the right flank of C56BL/6 male mice. Tumors were harvested on day 18. The single cell suspension was prepared, stained with the proper antibodies, followed by flow cytometry analysis.

*Tissue digestion, cell isolation and flow cytometry*

Thymus, spleen, mesenteric lymph nodes (mLN), and peripheral lymph nodes (pLN), were dissociated into a single-cell suspension and RBC lysis buffer (Biolegend) was used to remove red blood cells. To isolate tumor, tissues were dissected and incubated for 20 minutes at 37°C with collagenase D (1 mg/mL; Roche), dispase (0.05 U/mL; Worthington), and DNase I (100 mg/mL; SigmaAldrich). Digested tissue was then filtered through a 40-μm nylon strainer (VWR). Blood cells were removed with RBC lysis buffer (Biolegend). Cell suspension was washed by PBS.

For flow cytometry staining, cells were washed twice in FACS buffer and FcR blocking was applied 10 minutes at 4 °C. Live/dead staining was performed for 10 minutes at 4 °C with Fixable Viability Dye (Affymetrix) or live/dead blue (Thermofisher) before staining with the surface antibody (described below) mix for 30 minutes at 4 °C in FACS buffer. For intracellular staining, Foxp3/Transcription Factor Staining Buffer Set (eBioscience) was used according to the manufacturer's protocol. Cells were then incubated with antibodies for 1-3 hours in permeabilization buffer. Cells for cytokine production assessment were stimulated in T cell medium with anti-CD3 (1 μg/ml)/CD28 (5 μg/ml) for 5 hours at 37 °C then followed with FACS staining. Samples were analyzed immediately on BD FACSDiva, Fortessa or Cytek Aurora, and data analysis was performed using FlowJo (Tree Star) or OMIQ software.

For pSMAD2/3 staining, tissues were meshed in the fixation buffer (Invitrogen) for 30 minutes and filtered through a 40-μm nylon strainer (VWR). Cell suspensions were permeabilized in the perm buffer at room temperature (RT) for 30 minutes. Cell surface markers were stained at RT in FACS buffer for 1 hour. pSMAD2/3 and Foxp3 were stained overnight at 4 ℃ in FACS buffer. Flow cytometry was performed immediately using Cytek Aurora.

**Immune phenotyping panel:** Anti-CD45 (Clone 30-F11, Brilliant Violet 510, BioLegend), anti-CD3 (Clone 17A2, BUV737, BD Biosciences), anti-CD8a (Clone 53-6.7, BUV496, BD Biosciences), anti-CD4 (Clone RM4-5, APC/Fire™ 810, BioLegend), anti-Foxp3 (Clone FJK-16s, eFluor450, Invitrogen), anti-CD25 (Clone PC61.5, Super Bright 600, Invitrogen), anti-CD11b (Clone M1/70, Alexa Fluor 532, Invitrogen), anti-F4-80 (Clone T45-2342, BUV395, BD Horizon), anti-CD11c (Clone N418, Brilliant Violet 750, BioLegend), anti-MHC-II (Clone M1/42, BUV615, BD Biosciences), anti-NK-1.1 (Clone PK136, Brilliant Violet 570, BioLegend), anti-Ly-6C (Clone HK1.4, Brilliant Violet 605, BioLegend), anti-Ly-6G (Clone 1A8-Ly6g, Super Bright 436, Invitrogen), anti-CD103 (Clone 2E7, Brilliant Violet 711, BioLegend), anti-PD-1 (Clone J43, FITC, Invitrogen), anti-PD-L1 (Clone B7-H1, Brilliant Violet 421, BioLegend), anti-CD206 (Clone MR6F3, APC-eflour780, Invitrogen), anti-CD38 (Clone 90/CD38, PE/Cyanine7, BioLegend), anti-Arginase 1 (Clone A1exF5, Alexa Fluor 700, Invitrogen), anti-CD64 (Clone X54-5/7.1, APC, BioLegend), XCR1 (Clone ZET, PerCP/Cyanine5.5, BioLegend), anti-CD172 (Clone P84, PE/Dazzle™ 594, BioLegend), anti-CD19 (Clone 6D5, Spark NIR™ 685, BioLegend), anti-CD24 (Clone M1/69, BV480, BD Biosciences); **T cell exhaustion panel:** Anti-CD45 (Clone 30-F11, Brilliant Violet 510, BioLegend), anti-CD3 (Clone 17A2, BUV737, BD Biosciences), anti-CD8a (Clone 53-6.7, BUV496, BD Biosciences), anti-CD4 (Clone RM4-5, APC/Fire™ 810, BioLegend), anti-Foxp3 (Clone FJK-16s, eFluor450, Invitrogen), anti-CD25 (Clone PC61.5, Super Bright 600, Invitrogen), anti-TOX (Clone REA473, PE, Miltenyi Biotec), anti-CD44 (Clone IM7, BUV611, Invitrogen), anti-CD62L (Clone MEL-14, Brilliant Violet 421, BioLegend), anti-Slamf6 (Clone 13G3-19D, APC, Invitrogen), anti-PD-1 (Clone J43, APC-eflour780, Invitrogen), anti-Tim3 (Clone RMT3-23, Brilliant Violet 711, BioLegend), anti-Lag3 (Clone C9B7W, BUV 805, BD Biosciences), anti-Klrg1 (Clone 2F1, Pacific Orange, Invitrogen), anti-CD27 (Clone LG.3A10, BUV563, BD Biosciences), anti-CD38 (Clone 90/CD38, Brilliant Violet 750, BD Biosciences), anti-ICOS (Clone 7E.17G9, Super Bright 436, Invitrogen), anti-CD69 (Clone H1.2F3, PE/Cyanine7, BioLegend), anti-TIGIT (Clone 1G9, Brilliant Violet 650, BD Optibuild), anti-GITR (Clone MIH44, BUV615, BD Biosciences), anti-CTLA4 (Clone UC10-4B9, PE/Dazzle™ 594, BioLegend), anti-CD95 (Clone Jo2, BV480, BD Biosciences), anti-Ki67 (Clone B56, BUV395, BD Biosciences), anti-Tcf1 (Clone C63D9, PE/Cyanine5, Cell Signaling Technology), anti-Bcl-2 (Clone BCL/10C4, Alexa Fluor 647, BioLegend), anti-Granzyme B (Clone QA16A02, Alexa Fluor 700, BioLegend), anti-T-bet (Clone O4-46, Brilliant Violet 786, BD Biosciences); **Cytokine panel:** Anti-CD45 (Clone 30-F11, Brilliant Violet 510, BioLegend), anti-CD3 (Clone 17A2, BUV737, BD Biosciences), anti-CD8a (Clone 53-6.7, BUV496, BD Biosciences), anti-CD4 (Clone RM4-5, APC/Fire™ 810, BioLegend), anti-Foxp3 (Clone FJK-16s, eFluor450, Invitrogen), anti-CD11b (Clone M1/70, Alexa Fluor 532, Invitrogen), anti-TOX (Clone REA473, PE, Miltenyi Biotec), anti-Tcf1 (Clone C63D9, PE/Cyanine7, Cell Signaling Technology), anti-TNFα (Clone MP6-XT22, Percp-eflour 710, Invitrogen), anti-IFNγ (Clone XMG1.2, Brilliant Violet 786, BD Biosciences), anti-Granzyme B (Clone QA16A02, Alexa Fluor 700, BioLegend), anti-Perforin (Clone eBioOMAK-D, FITC, Invitrogen), anti-IL-2 (Clone JES6-5H34, PE-eflu610, Invitrogen), anti- IL-4 (Clone 11B11, BV605, BD Horizon), anti-IL-10

(Clone JES5-16E3, APC, Invitrogen), anti-IL-17A (Clone TC11-18H10, APC-Cy7, BD Pharmingen), anti-IL-21 (Clone FFA21, eFluor660, Invitrogen); **phospho-flow panel:** Anti-CD45 (Clone 30-F11, Brilliant Violet 510, BioLegend), anti-CD3 (Clone 17A2, BUV737, BD Biosciences), anti-CD8a (Clone 53-6.7, BUV496, BD Biosciences), anti-CD4 (Clone RM4-5, APC/Fire™ 810, BioLegend), anti-Foxp3 (Clone FJK-16s, eFluor450, Invitrogen), anti-CD25 (Clone PC61.5, Super Bright 600, Invitrogen), anti-CD11b (Clone M1/70, Alexa Fluor 532, Invitrogen), anti-F4-80 (Clone T45-2342, BUV395, BD Horizon), anti-CD11c (Clone N418, Brilliant Violet 750, BioLegend), anti-MHC-II (Clone M1/42, BUV615, BD Biosciences), anti-NK-1.1 (Clone PK136, Brilliant Violet 570, BioLegend), anti-Ly-6C (Clone HK1.4, Brilliant Violet 605, BioLegend), anti-Ly-6G (Clone 1A8-Ly6g, Super Bright 436, Invitrogen), anti-CD206 (Clone MR6F3, APC-eflour780, Invitrogen), anti-CD19 (Clone 6D5, Spark NIR™ 685, BioLegend), anti-pSMAD2/3 (Clone O72670, PE, BD Pharminen)

*Multiplex immunofluorescence analysis*

The samples were outsourced to Fred Hutch for the IF staining and the method was provided by Fred Hutch. Formalin-fixed paraffin-embedded tissues were sectioned at 4 microns and baked for 1h at 60 °C. The slides were dewaxed by using dewax solution (Leica). Antigen retrieval (Bond Wash Solution) was applied at 100 °C for 20 mins.

| Position | Antibody | Clone/ Host | Manufacturer/ Catalog Number | Dilution | Secondary | Opal Dye |
|---|---|---|---|---|---|---|
| 1 | cd45 lca | Rabbit polyclonal | Abcam ab10558 | 1:3000 | PowerVision Rabbit HRP | Opal 520 |
| 2 | SMA | Rabbit polyclonal | Proteintech 80008-1-RR | 1:5000 | PowerVision Rabbit HRP | Opal 540 |
| 3 | cd8a | Rabbit D4W2Z | Cell signaling 98941 | 1:1500 | PowerVision Rabbit HRP | Opal 570 |

3% $H_2O_2$ was used for endogenous peroxidase blocking for 5 mins followed by incubating 10% normal mouse serum in TCT buffer (0.05M Tris, 0.15M NaCl, 0.25% Casein, 0.1% Tween 20, pH 7.6) for 10 mins. CD45 lca antibody was applied for 1h and the secondary antibody was stained for 10 mins. Then, the tertiary TSA-amplification reagent was applied (PerkinElmer OPAL fluor) for 10 mins. After secondary and tertiary application, a high stringency wash was performed by using high-salt TBST solution (0.05M Tris, 0.3M NaCl, and 0.1% Tween-20, pH 7.2-7.6). Polymer HRP as secondary was indicated in the table (Leica).

SMA staining was done after stripping process in retrieval solution for 20 mins at 100 °C. Before SMA staining, 3% $H_2O_2$ was used for endogenous peroxidase blocking. The process CD8a staining was repeated as SMA. Lastly, slides were stained with DAPI for 5 minutes, rinsed and coverslipped in Prolong Gold Antifade reagent (Invitrogen).

Images were acquired on the Perkin Elmer Vectra 3.0 Automated Imaging System (Akoya Biosciences, Marlborough, MA) using the filters and exposure times in the table below.

| Filter | Scan exposure time [2]: | Field exposure time [2]: |
|---|---|---|
| DAPI | 25 | 200 |
| FITC | 150 | 250 |
| CY3 | 30 | 70 |
| Texas Red | 25 | 40 |
| CY5 | 150 | 200 |

Briefly, the slides were first scanned using long pass filters at 10x magnification to capture the entire tissue section. These images were annotated for the Regions of Interests (ROIs) covering

the entire tissue. Next, these ROIs were imaged using multispectral imaging settings for each biomarker. The resulting .im3 multispectral images were quantified for CD45, CD8a, SMA and DAPI. These ROIs were imported into the inForm software for further analyses. First, the images were annotated for biomarkers and fluorophores. The autofluorescence signal was isolated and the multiplexed fluorescence signals were unmixed. The images were normalized to the exposure time. The inForm software allows development of machine-learning based segmentation of tissues categories and segmentation of cells. A subset of ROIs was sampled to make training set for image processing, tissue segmentation, cell segmentation and phenotyping algorithms. These algorithms were applied to all ROIs of all images in the dataset for batch analyses. The resulting comprehensive data that was further analyzed using phenoptr package and R-programming for identifying and quantifying cells for each biomarker within each tissue compartment (defined as tumor and stroma) as well as in the entire tissue section.

*Region Definitions*

The imaged cells were classified into stromal or tumor cell categories by a machine learning algorithm (inform software from Akoya). Next, we determined the largest cluster of tumor cells by using a flood-fill algorithm in the following way. The region was discretized into a square lattice with lattice constant 30μm where a pixel is considered occupied if at least one tumor cell is present in it. The occupied pixels were connected to form clusters by joining face sharing nearest neighbors. We calculated the convex hull of the largest cluster of tumor cells to define the boundary between the tumor mass and the exterior stromal region. The center of mass of the tumor was calculated by taking the average position of all the tumor cells in the largest cluster of tumor cells. We then use the boundary between tumor mass and the stromal region and the center of mass of largest cluster of tumor cells to divide the tumor region into three regions (Intermediate I, Intermediate II, and Interior) (**Fig. S6A**) based on their proximity to the center of mass in the following way. If $\{x_i^{(b)}, y_i^{(b)}\}$ represent the positions of the tumor cells in the boundary where the center of mass is the origin, then the boundary of a region in the tumor mass is given by $\{\alpha x_i^{(b)}, \alpha y_i^{(b)}\}$, where $\alpha<1$. The α values corresponding to the boundaries are shown in **Fig. S6A**. The spatial distributions of $CD8^+$ T cells and other cells were analyzed in these regions to evaluate the changes in the organization of these cells based on the proximity of the cells to the center of the tumor region.

*Density*

Density (σ) of a particular cell type, e.g., $CD8^+$ T cell, in a region is calculated by the ratio of the total number ($N_{Tot}$) of the cells and the area ($A$) of that region, i.e., $\sigma = \frac{N_{Tot}}{A}$. The area of a region is calculated numerically by partitioning the region (e.g., Intermediate II) into a square lattice with lattice constant $a = 30\ \mu m$ and then calculating the area of the filled portion of the lattice.

*Two-Point Correlation*

We compute spatial two point correlation for $CD8^+$ T cells in a region (e.g., Intermediate II) in the following way (see [3] page 34 for more on the two point correlation). For any $CD8^+$ T cell (indexed by $i$) in the region, we draw an annular region of radius $r$ and thickness δ (= 3μm) with the $CD8^+$ T cell positioned at the center and compute the density of other $CD8^+$ T cells in that annular region (**Fig. S6B**). Defining $n_{i,(r-\delta/2,r+\delta/2)}$ as the number of $CD8^+$ T cells in the annulus and $A_{annulus}$ as the area of the annular region, the density $\sigma_i(r)$ of the $CD8^+$ T cells in the annular region surrounding the $i$th $CD8^+$ T cell is given by,

$$\sigma_i(r) = \frac{n_{i,\left(r-\frac{\delta}{2},r+\frac{\delta}{2}\right)}}{A_{Annulus}},$$

where $A_{annulus}=\pi r\delta$. The total number ($N_{CD8+}$) of $CD8^+$ T cells and density of the $CD8^+$ T cells ($\sigma_{CD8+} = N_{CD8+}/$(area of the region)) in the region is also computed. The pair correlation function is then given by,

$$C(r) = \frac{1}{N_{CD8^+}} \sum_i \sigma_i(r) \; - \; \sigma_{\mathrm{CD8^+}}$$

This calculation is done for multiple radii r and the resulting function is plotted as a function of *r*.

*Bulk RNA-seq analysis*

Public data access and analysis.
The bulk RNA-seq data of bladder cancer [4] were downloaded from http://research-pub.gene.com/IMvigor210CoreBiologies/, in support of survival analysis and *LRRC32* gene expression analysis. The 167 bladder tumor samples were selected based on the "Best Confirmed Overall Response" annotation, including 15 CR (complete response), PR (partial response), SD (stable disease), and PD (progressive disease). *LRRC32-TGFB* related signature includes: *LRRC32*, *ITGB6*, *ITGB8*, *ITGAV*, *ITGA2B*, *SELP*, *F2*, *TGFB1* genes. The DESeq 2 (v.1.30) normalization method was applied before the survival analysis and *GARP* gene expression. The survival analysis was performed based on the package survival (v 3.1).

*Samples and library preparation*

$1x10^5$ MB-49 cells were injected s.c. on the right flank of *hLRRC32*$^{KI}$ male mice. PIIO-1 (200 μg/mouse, i.p.) were delivered on day 6 and 9 for 2 doses. Tumors were collected on day 10. Single cell suspension and RNA isolation were prepared. Total RNA was isolated by using RNeasy Kits (Qiagen) and then subjected to bulk RNA sequencing. RNA quality was verified with an Agilent Bioanalyser. Libraries were prepared using NEBNext Ultra TM RNA Library Prep Kit for Illumina (NEB, USA), following manufacturer's recommendations.

*Alignment and quantification*

Sequencing was outsourced to Macrogen and performed on an Illumina Hiseq6000 with the following requirement: 150 pb of read length, paired-end reads, and 300 M reads/sample. The reads were removed if they contained adapters, N was greater than 10% (N represents a base that could not be determined), or they were identified as low-quality reads in which the Q score (Quality value) was less than 5. Filtered reads were then aligned to the GRCm38 mouse genome using the Hisat2 (v.2.0.5) followed default settings, and read counts were determined with the featureCounts (v1.5.0-p3) software. Raw read counts were normalized using the DESeq2 package with default settings.

*Pathway enrichment analysis and deconvolution analysis*

The DEGs were selected if the *p*-value were less than 0.001 and the absolute value of log-fold change was higher than 0.5 [5]. Based on the identified DEGs, the enrichment analyses of GO terms (Biological Process, Cell Component, and Molecular Function) were performed via the R package clusterProfiler (v.3.18.0) [6]. GSEA (v.4.0.3) was also implemented for enrichment

analysis and visualization [7] . The deconvolution was performed using TIMER 2.0 following its tutorial [8].

*Immunohistochemistry (IHC)*

Mouse tumor slides were processed, and antigen retrieved as describes previously[1]. For mouse IHC, tissues were collected and place into 4% paraformaldehyde overnight for fixation, then fixed tissue was incubated in 70% ethanol overnight prior to paraffin embedding, and then cut for hematoxylin and eosin (H&E) staining. For pSMAD2/3 or α-SMA on paraffin tumor sections, 4 μm sections were incubated with 3% $H_2O_2$. To minimize nonspecific staining, sections were incubated with the appropriate animal serum for 20 min at RT, followed by incubation with primary anti-pSMAD2/3 antibody (Abcam) or α-SMA (Abcam) overnight at 4 °C. Staining with secondary antibodies (Vectastain ABC Kit) was then performed before development using DAB substrate (Vector Labs SK-4100). The staining intensity of pSMAD2/3 or α-SMA was graded as follows with the sample identity blinded (0: negative; 1: faint; 2: moderate; 3: strong but less intense than 4; and 4: intense).

*Soluble TGFβ1 ELISA*

Mouse blood was collected in Eppendorf tubes. Sera were collected after coagulation for 1 hour at RT and centrifugation at 5,000 rpm for 15 minutes. Capture ELISA for TGFβ1 was performed according to manufacturer instructions (BioLegend). Active TGFβ1 was measured with no additional manipulation. Total TGFβ1 was measured following acidic activation using 1 M HCl for 10 min at RT, and neutralization with 1.2N NaOH. Active TGFβ1 and total TGFβ1 levels were measured using TGFβ1 ELISA kits according to the manufacturer's protocols.

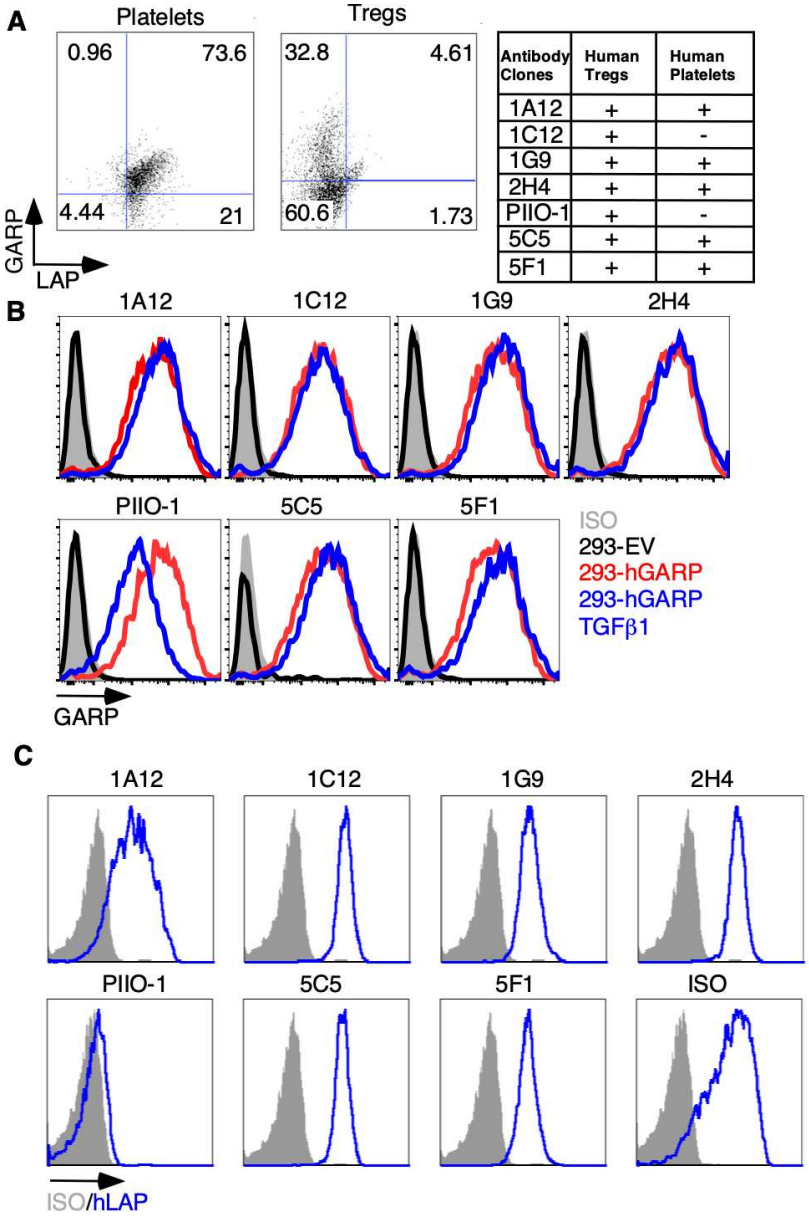


| Antibody Clones | Human Tregs | Human Platelets |
|---|---|---|
| 1A12 | + | + |
| 1C12 | + | - |
| 1G9 | + | + |
| 2H4 | + | + |
| PIIO-1 | + | - |
| 5C5 | + | + |
| 5F1 | + | + |

**Supplementary figure 1.** ***In vitro*** **characterization of anti-GARP antibodies. A.** GARP expression on human regulatory T cells and platelets was evaluated by flow cytometry with multiple clones of anti-GARP antibodies at 10 μg/ml. Representative flow plots were shown (*left*). Cell types with their GARP expression recognized by different clones was summarized in the table (*right*). **B.** 293FT cell line was transfected with empty vector (EV), human GARP (hGARP) only or co-transfected with hGARP and latent TGFβ1. GARP expression on indicated cell line was detected by flow cytometry with anti-GARP antibodies at 10 μg/ml. **C.** Stable hGARP-expressing Jurkat cell line was incubated with recombinant LTGFβ1 together with isotype control or anti-GARP antibodies at 10 μg/ml for 30 min at 37 ℃. Human LAP expression level was detected by flow cytometry. This data represents 2-6 independent experiments.

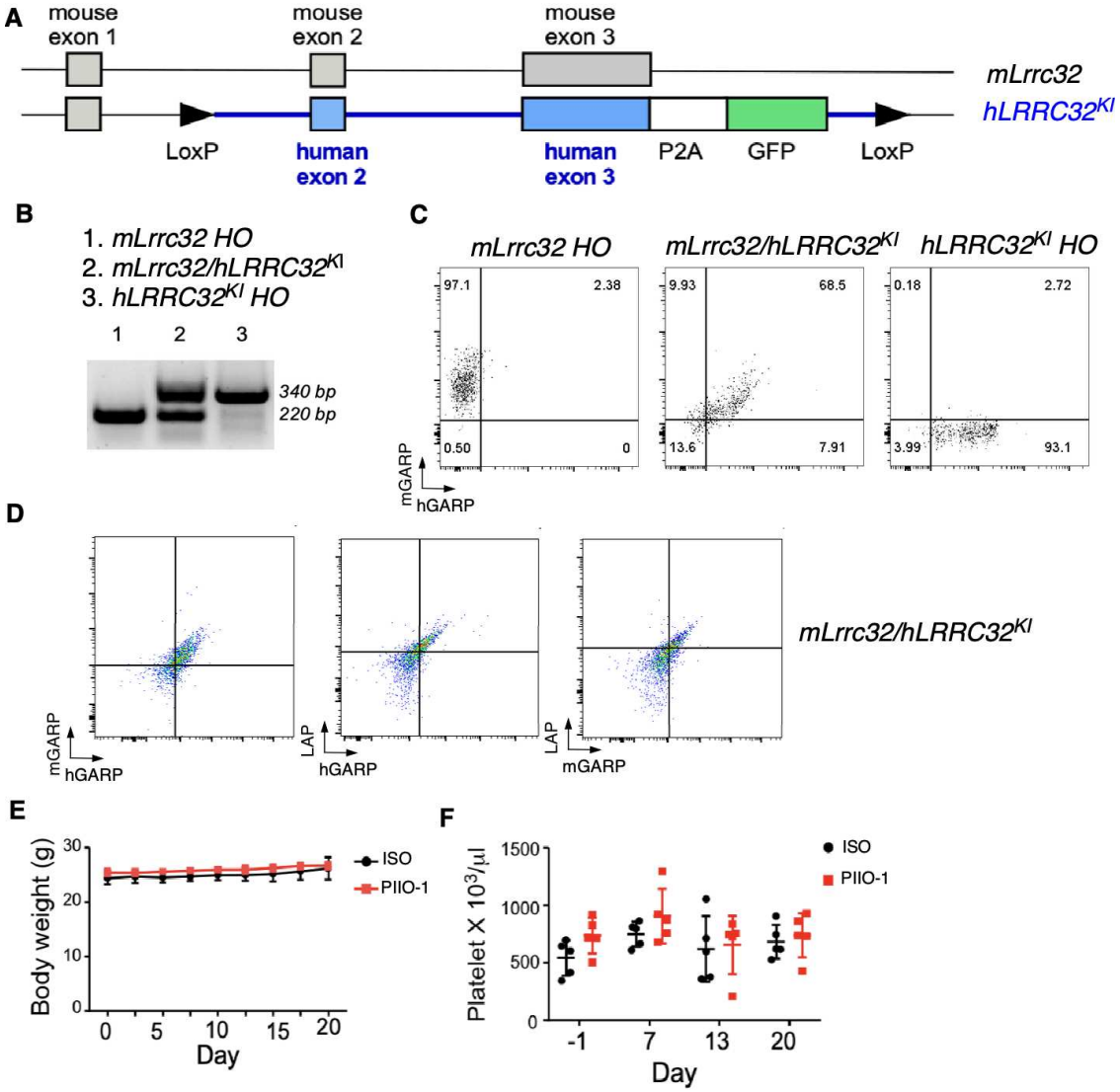


**Supplementary figure 2. Generation of human *LRRC32* knock-in mice. A.** The scheme of construct design. *mLrrc32* indicates mouse allele. *hLRRC32*$^{KI}$ denotes human *LRRC32* knock-in allele. **B.** PCR confirmation of genotypes of the indicated mice. HO, homozygous. **C.** GARP expression on CD41$^{+}$ platelets from indicated mice was detected by commercial mGARP and hGARP flow antibody. **D.** Binding ability between human and mouse GARP to LAP on CD41$^{+}$ platelets was compared. GARP and LAP expression on CD41$^{+}$ platelet from indicated mouse were detected by flow cytometry. **E.** and **F**. Toxicity study of PIIO-1. *hLRRC32*$^{KI}$ mice (n=5/group) were injected i.p. with 200 μg mIgG1 or PIIO-1 twice per week (n=5/group) for 6 doses. Body weight and peripheral blood platelet levels were measured.

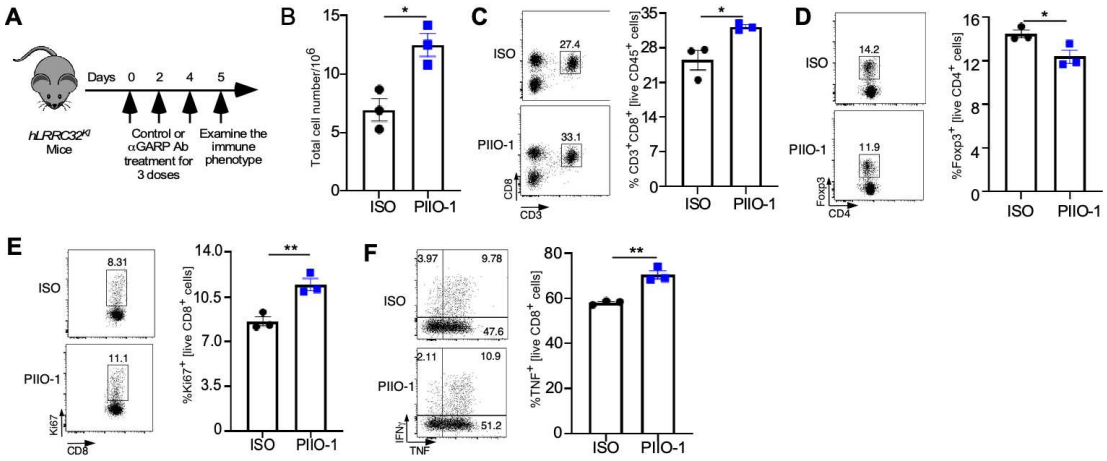


**Supplementary figure 3. Systemic administration of PIIO-1 to *hLRRC32$^{KI}$* mice increases peripheral LN cellularity including CD8$^+$ T cells and their function. A.** *hLRRC32$^{KI}$* mice were injected i.v. with 200 μg/mouse PIIO-1 or mIgG1 every 48 hours for a total of 3 injections. Mice were sacrificed and peripheral lymph nodes were harvested 24 hours after the 3$^{rd}$ injection of PIIO-1. **B.** Absolute number of live cells from peripheral lymph nodes. **C-E.** Flow cytometric analysis of peripheral lymph node examining the frequency of, **C.** CD3$^+$CD8$^+$ T cells, **D.** Ki67$^+$ CD8$^+$ T cells, and **E.** Foxp3$^+$ regulatory T cells. **F.** Percentage of IFNγ and TNFα producing CD8$^+$ T cells by intracellular staining. N=3 per group, data representative of two independent experiments. Two-tailed Student's t test was used for statistics. Data presented as mean +/- SEM. *p<0.05, **p<0.01.

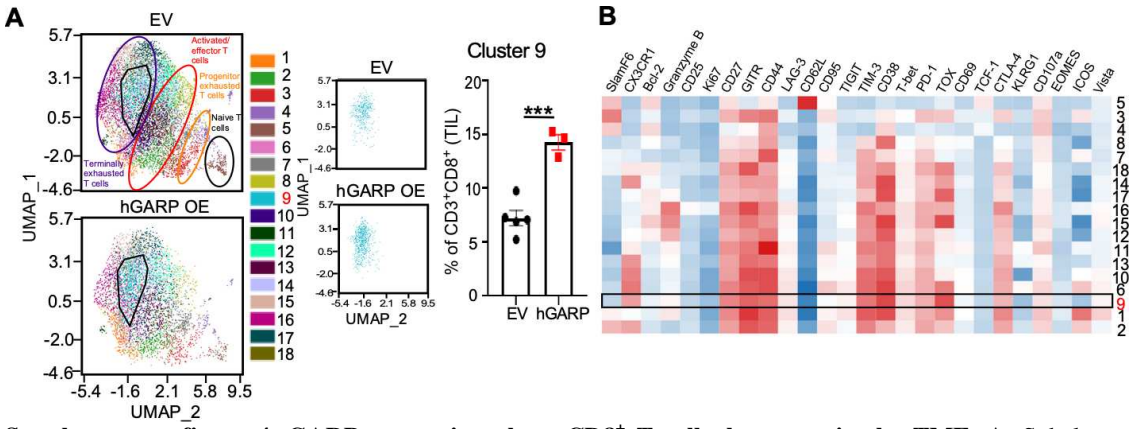


**Supplementary figure 4. GARP expression alters CD8$^+$ T cell phenotype in the TME**. **A.** Subcluster analysis of tumor-infiltrating CD8$^+$ T cells in EV vs hGARP over-expressing MB-49 tumor. 1x10$^5$ MB-49-EV or hGARP cells were injected into C57BL/6 mice s.c. and tumors were harvested on day 18. UMAP dimension reduction of tumor-infiltrating CD8$^+$ T cells was done after staining with 33 markers and spectral flow cytometry analysis. Shown is the data gated on live CD45$^+$CD3$^+$CD8$^+$ T cells, subsampled on 5000 cells per sample. Unsupervised clustering analysis was performed using FlowSOM algorithm with an elbow method approach for cluster number determination. **B.** Heatmap of **A** showing expression levels of indicated markers by each cluster. Cluster difference was measured by two-tailed Student's t test. Data presented as mean +/- SEM. *** p<0.001.

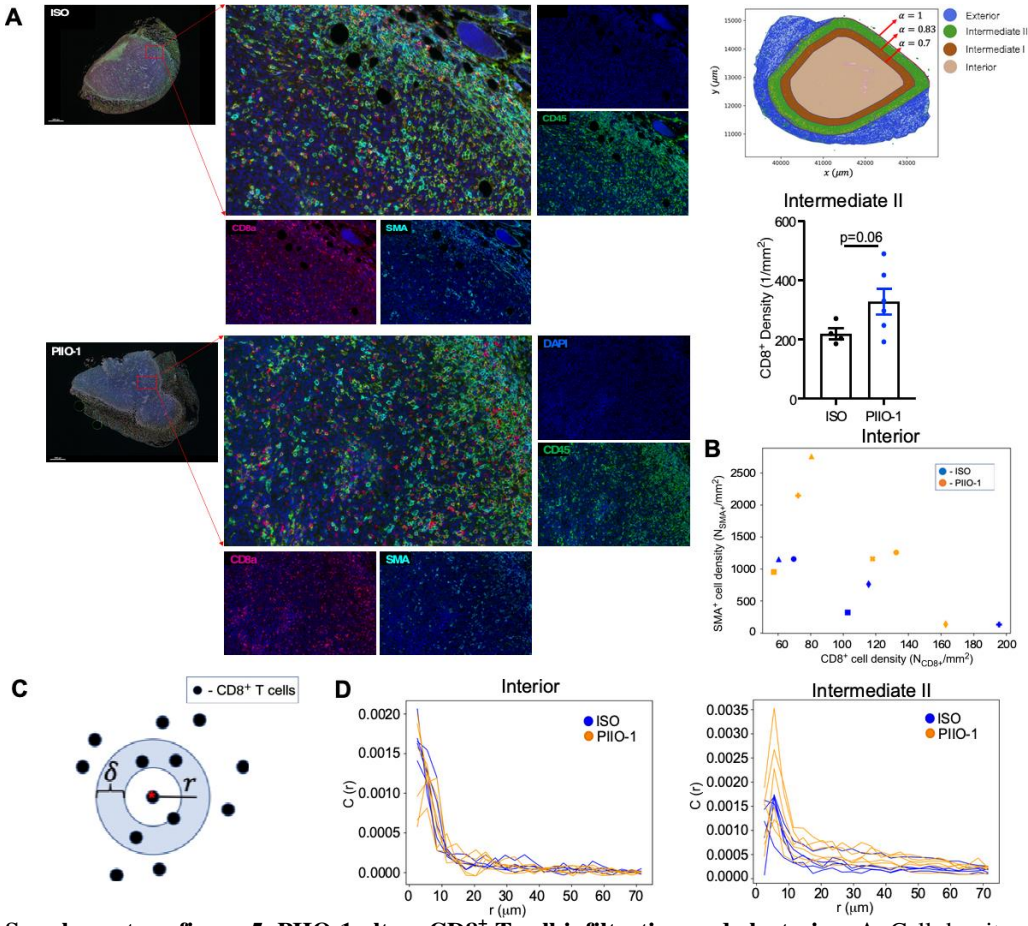


**Supplementary figure 5. PIIO-1 alters CD8$^+$ T cell infiltration and clustering. A.** Cell density analysis of tumor-infiltrating CD8$^+$ T cells in MB-49 tumor treated with mIgG1 or PIIO-1. 1×10$^5$ MB-49 cells were injected s.c. on the right flank of *hLRRC32$^{KI}$* male mice. PIIO-1 or ISO was delivered (200 μg/mouse, i.p.) on days 6 and 9. Tumors were collected on day 10 and multiplex IF analysis was performed on histology samples of the tumors. (*Left*) Histology samples were stained with CD45, CD8, SMA, DAPI. (*Upper right*) Shows tumor regions defined for computational analysis. The boundary at α=1 denotes the boundary between the stromal and the tumor region. This boundary was scaled down by α to create additional tumor regions (see supplemental methods for further details). (*Lower right*) CD8$^+$ T cell density was quantified in the regions defined in (A) for ISO and the PIIO-1 treated. PIIO-1 treatment increased CD8$^+$ T cell density in the intermediate II region compared to ISO. **B.** Co-dependence of the densities of SMA$^+$ and CD8$^+$ T cells in the interior region defined in (A). Densities obtained from slides from different mice are shown with different symbols. The magnitude of the negative correlation between the SMA$^+$ and CD8$^+$ T cells in the ISO (Corr= -0.86) decreases when the tumor is treated with PIIO-1 (Corr= -0.62). **C**. Core steps used in the calculation of the two point correlation function where the density of CD8$^+$ T cells in an annular region of radius *r* and thickness $\delta$ corresponding to a CD8$^+$ T cell at the center is calculated (see supplemental methods for further details). **D.** Variation of the two point correlation function C(r) with the distance *r* for the CD8$^+$ T cells in the interior (*left*) and the intermediate II (*right*) tumor regions for tumors in ISO and PIIO-1 treated mice. Multiple curves in the same color show the data for C(r) obtained from different slides in different mice (ISO or PIIO-1 treated). The data shows that C(r) has larger peaks at r≈ 7 μm for the PIIO-1 treated compared to ISO in the intermediate II region. This indicates increased grouping of CD8$^+$ T cells within a length scale of 7 μm in the intermediate II region when treated with PIIO-1. Cell density difference measured by Welch's t test. Data presented as mean +/- SEM.

**A**

| | ISO | PIIO-1 | anti-PD-1 | Combo |
|---|---|---|---|---|
| Total number | 5 | 5 | 7 | 7 |
| Tumor sizes % (N) | | | | |
| Uncontrolled growth * | 40% (2) | 40% (2) | 57.1% (4) | 0% (0) |
| p Value | | | **** | |

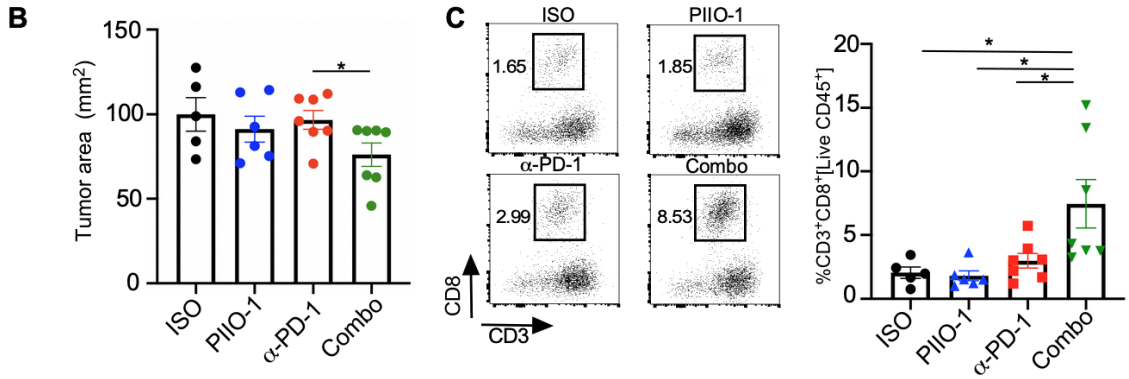


**Supplementary figure 6. PIIO-1 overcomes resistance to PD-1 blockade in LLC and CMT-167 models and promotes CD8$^+$ T cell infiltration. A**. Summary of number of mice in each treatment group with uncontrolled tumors (> 115 mm$^2$ on day 17). 5x10$^5$ LLC cells were injected s.c. on the right flank of *hLRRC32$^{KI}$* female mice, followed by treatment with ISO, PIIO-1, PD-1 or combination. Treatments were delivered on day 8 after tumor inoculation and every 3 days thereafter for a total of 4 doses. **B**. Tumor volume 18 days after s.c. injection of 1x10$^5$ CMT-167 cells. Mice were treated with 4 injections of indicated antibody (day 8, 11, 14 and 17). **C.** Frequency of tumor-infiltrating CD8$^+$ T cells of day 18 CMT-167 tumors (*left*-representative flow plots gated on CD45$^+$ cells; *right* – data quantification). Data from A is analyzed by two-tailed Fisher's exact test. Other data is analyzed by two-tailed Student's t test. All data are presented as mean ± SEM. * p <0.05, **** p<0.0001.

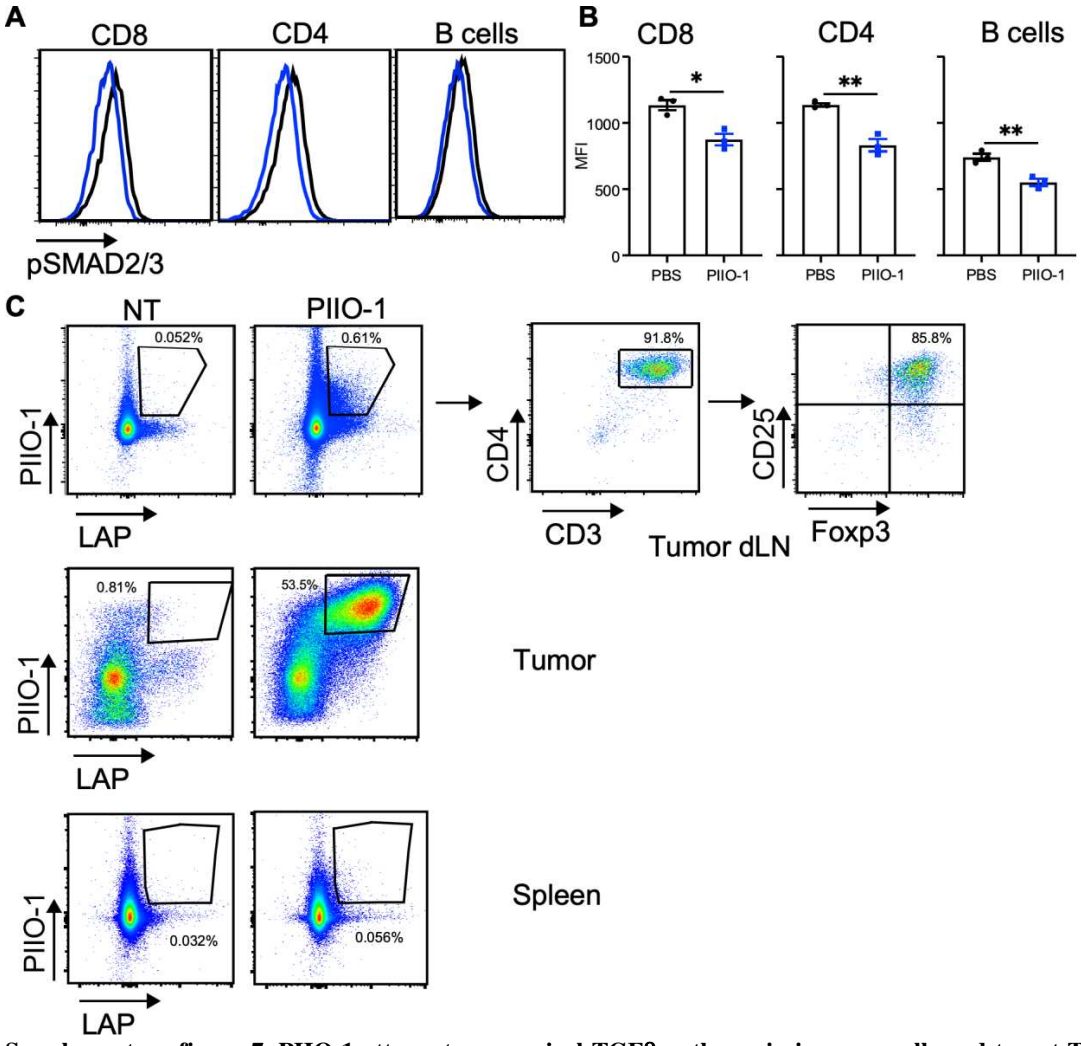


**Supplementary figure 7. PIIO-1 attenuates canonical TGFβ pathway in immune cells and target Tregs primarily in the dLN. A.** 1x10$^5$ MB-49 cells were injected s.c. in the right flank of *hLRRC32*$^{KI}$ male mice. Humanized PIIO-1 (200 μg/mouse, i.p.) was administered on days 18 and 20. dLNs were collected on day 21, then isolated and stained for intracellular pSMAD2/3 with cell linage markers (see supplemental methods for further details), followed by flow cytometry analysis. pSMAD2/3 expression level in cells from dLN was shown. **B.** Quantification of panel A. **C.** 1x10$^5$ MB-49 cells were injected s.c. in the right flank of *hLRRC32*$^{KI}$ male mice. Humanized PIIO-1 (200 μg/mouse, i.p.) was administered on day 18. Tumor dLNs, tumor and spleen were collected on day 19. Humanized PIIO-1 was detected by anti-human Fc flow antibody. Humanized PIIO-1 and LAP co-expressed cells were gated and further analyzed for cell identity. Data was performed using two-tailed Student's t test and presented as mean+/-SEM. * p <0.05, ** p<0.01.

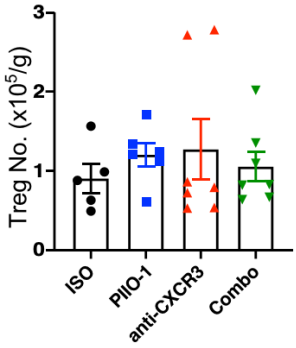


**Supplementary figure 8. Anti-CXCR3, with or without anti-GARP antibody PIIO-1 does not alter Treg numbers in the TME.** $1x10^5$ MB-49 cells were injected s.c. in the right flank of *hLRRC32*$^{KI}$ male mice. Humanized PIIO-1 and anti-CXCR3 antibody were administered (200 µg/mouse, i.p.) every 3 days for a total of 4 treatments starting on day 5. Absolute number of Treg cells in the tumor was then quantified by flow cytometry, based on live gating of TILs with the following phenotype: $CD45^+CD3^+CD4^+CD25^+Foxp3^+$. Data are presented as mean+/-SEM. No significant difference between groups was observed based on two-tailed Student's t test,.

**Reference:**

1. Metelli A, Wu BX, Fugle CW, et al. Surface Expression of TGFbeta Docking Receptor GARP Promotes Oncogenesis and Immune Tolerance in Breast Cancer. *Cancer Res* 2016;76(24):7106-17. doi: 10.1158/0008-5472.CAN-16-1456
2. Pender A, Titmuss E, Pleasance ED, et al. Genome and Transcriptome Biomarkers of Response to Immune Checkpoint Inhibitors in Advanced Solid Tumors. *Clin Cancer Res* 2021;27(1):202-12. doi: 10.1158/1078-0432.CCR-20-1163 [published Online First: 2020/10/07]
3. Chaikin PM, Lubensky TC. Principles of condensed matter physics. Cambridge ; New York, NY, USA: Cambridge University Press 1995.
4. Mariathasan S, Turley SJ, Nickles D, et al. TGFbeta attenuates tumour response to PD-L1 blockade by contributing to exclusion of T cells. *Nature* 2018;554(7693):544-48. doi: 10.1038/nature25501 [published Online First: 2018/02/15]
5. Alberti C, Manzenreither RA, Sowemimo I, et al. Cell-type specific sequencing of microRNAs from complex animal tissues. *Nat Methods* 2018;15(4):283-89. doi: 10.1038/nmeth.4610 [published Online First: 2018/02/27]
6. Yu G, Wang LG, Han Y, et al. clusterProfiler: an R package for comparing biological themes among gene clusters. *OMICS* 2012;16(5):284-7. doi: 10.1089/omi.2011.0118 [published Online First: 2012/03/30]
7. Subramanian A, Tamayo P, Mootha VK, et al. Gene set enrichment analysis: a knowledge-based approach for interpreting genome-wide expression profiles. *Proc Natl Acad Sci U S A* 2005;102(43):15545-50. doi: 10.1073/pnas.0506580102 [published Online First: 2005/10/04]
8. Li T, Fu J, Zeng Z, et al. TIMER2.0 for analysis of tumor-infiltrating immune cells. *Nucleic Acids Res* 2020;48(W1):W509-W14. doi: 10.1093/nar/gkaa407 [published Online First: 2020/05/23]